Proceedings of ICRC 2001: 2088 © Copernicus Gesellschaft 2001

ICRC 2001

Numerical studies of cosmic ray injection and acceleration

H. Kang[1], **T. W. Jones**[2], **and U. D. J. Gieseler**[3]

[1]Pusan National University, Pusan, Korea
[2]University of Minnesota, Minneapolis, USA
[3]Universität Siegen, Siegen, Germany

Abstract. We have developed a numerical scheme that incorporates a self-consistent cosmic-ray (CR hereafter) injection model into the combined gas dynamics and CR diffusion-convection code. Our hydro/CR code is designed to follow in a very cost-effective way the evolution of CR modified shocks by adopting subzone shock-tracking and multi-level adaptive mesh refinement techniques. The injection model is based on recent calculations of Malkov (1998) that considered the interactions of the suprathermal particles with self-generated MHD waves in quasi-parallel shocks. In this model, the particle injection is realized by filtering the diffusive flux of suprathermal particles across the shock to the upstream region according to a velocity-dependent transparency function, which represents the fraction of leaking particles. Thus, with this new code, we can eliminate a need to assume an injection rate as a free parameter. We have studied the CR injection and acceleration efficiencies for a wide range of shock Mach numbers and will discuss the preliminary results.

1 Introduction

According to quasi-linear theory as well as plasma simulations of strong quasi-parallel shocks, the streaming motion of the CR particles against the background fluid can induce wave generation via the cyclotron resonance leading to strong MHD waves that scatter particles and prevent them from leaking upstream (e.g., Bell 1978;Quest 1988). Hence only a small fraction of suprathermal particles can swim upstream against the wave-particle interactions and be injected into the CR population. This so-called "thermal leakage" injection process is important to reaching an understanding of the efficiency of diffusive shock acceleration (DSA) of the CRs. Malkov (1998) presented a self-consistent, analytic, nonlinear calculations for ion injection based on this process. The resulting theory has only one parameter; namely, the intensity of the downstream waves, and that is tightly restricted, both by the theory and by comparison with hybrid plasma simulations. By adopting Malkov's analytic solution, a numerical treatment of this injection model has been devised and incorporated into the combined gas dynamics and the CR diffusion-convection code (Gieseler et al., 2000). According to the Gieseler et al. (2000) simulations, the injection process seems to be self-regulated in such a way that the injection rate reaches and stays at a nearly stable value after quick initial adjustment, but well before the CR shock reaches a steady state structure. They found that about 10^{-3} of incoming thermal particles are injected into the CRs, roughly independent of Mach numbers. Due to severe computational requirement, however, their simulations were carried out only until the maximum momentum of $(p_{\rm max}/m_{\rm p}c) \sim 1$ was achieved. Since strong shocks are still evolving at the end of the simulations, the time asymptotic limit could not be estimated for either the CR acceleration efficiency or the CR spectrum.

The diffusion-convection equation for nonlinear DSA includes an extremely wide range of length scales for a Bohm type diffusion where scattering length is proportional to the particle momentum. Since the length and time scales for evolution of the CR kinetic equation scale directly with the diffusion coefficient, an accurate solution to the problem requires that one include all of those scales in the simulation, beginning just outside the gas subshock thickness. Thus we have developed a new CR shock code that can perform kinetic simulations with a strong momentum-dependent diffusion in a very cost-effect way (Kang et al. 2001). This code uses sub-zone shock tracking (LeVeque and Shyue, 1995) and multi-level adaptive mesh refinement techniques (Berger and LeVeque, 1998) to provide enhanced spatial resolution around shocks at modest cost compared to the coarse grid and vastly improved cost effectiveness compared to a uniform, highly refined grid.

The numerical method for the self-consistent injection model of Gieseler et al. (2000) has been implemented into this

Correspondence to: H. Kang
(ang@uju.es.pusan.ac.kr)

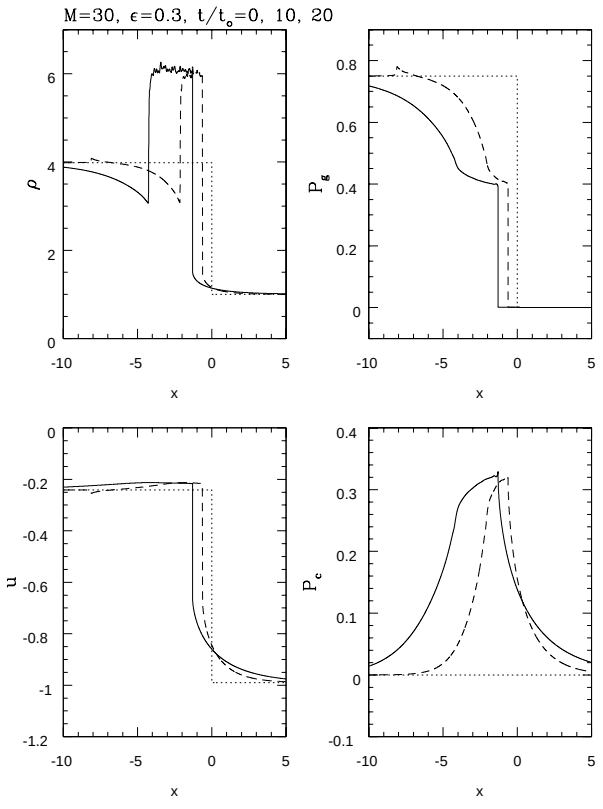

Fig. 1. Structure of $M = 30$ shock at $t/t_o = 0$ (dotted), 10 (dashed) and 20 (solid line). Five levels of refinements ($l_{\max} = 5$) were used.

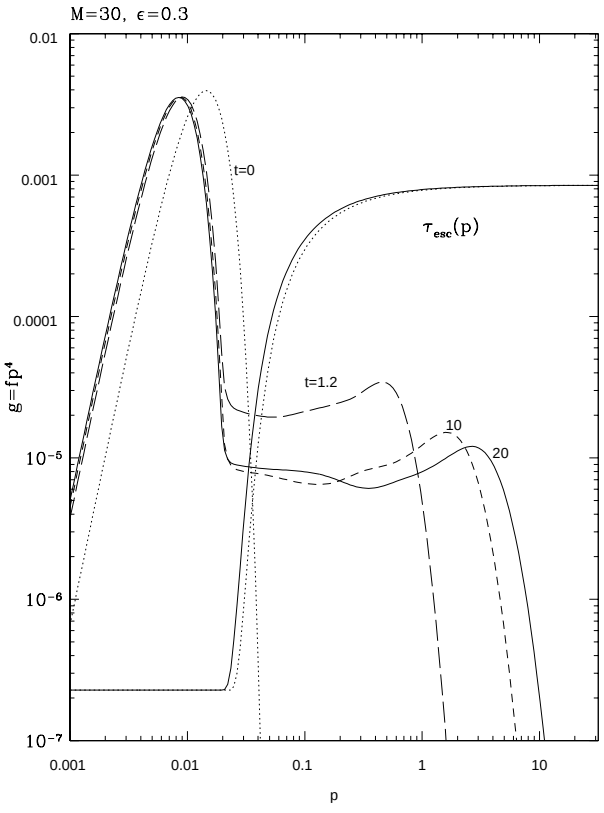

Fig. 2. Distribution function $g = p^4 f$ at $t/t_o = 0$ (dotted), 1.2 (long dashed), 10 (dashed), and 20 (solid line) for $M = 30$ and $\epsilon = 0.3$. The transparency function is shown at $t/t_o = 0$ (dotted line) and 20 (solid line).

CR/AMR code. With our new code we have calculated the CR injection and acceleration efficiency for shocks of different Mach numbers. In the present contribution we report the preliminary results.

2 CR/AMR hydrodynamics code

In order to follow accurately the evolution of a CR modified shock, it is necessary to resolve the precursor structure upstream of the subshock and, at the same time, to solve correctly the diffusion of the low energy particles near the injection pool. So a large dynamic range of resolved scales is required for CR shock simulations. To solve this problem generally we have successfully combined a powerful "Adaptive Mesh Refinement" (AMR) technique (Berger and LeVeque, 1998) and a "shock tracking" technique (LeVeque and Shyue, 1995), and implemented them into a hydro/CR code based on the wave-propagation method (Kang et al., 2001). The AMR technique allows us to "zoom in" inside the precursor structure with a hierarchy of small, refined grid levels applied around the shock. The shock tracking technique tracks hydrodynamical shocks within regular zones and maintains them as true discontinuities, thus allowing us to refine the region around the shock at an arbitrary level. The result is an enormous savings in both computational time and data storage over what would be required to solve the problem using more traditional methods on a single fine grid. It can provide a powerful numerical tool to study the CR injection and acceleration at astrophysical shocks.

3 Injection Model

In "thermal leakage" injection model, most of downstream thermal protons would be confined by the waves and only particles with higher velocity in the tail of the Maxwellian distribution are able to leak through the shock. In order to include self-consistently the injection of the CR protons according to the analytic solution of Malkov (1998), we have adopted the "transparency function" $\tau_{\rm esc}(v, u_2)$, which expresses the probability that supra-thermal particles at a given velocity can leak upstream through the magnetic waves, based on non-linear particle interactions with self-generated waves. In this scheme, the transparency function is approximated by

$$\tau_{\rm esc}(v,u_2) \;=\; H\left[\tilde{v}-(1+\epsilon)\right]\left(1-\frac{u_2}{v}\right)^{-1}\left(1-\frac{1}{\tilde{v}}\right) \cdot \exp\left\{-\left[\tilde{v}-(1+\epsilon)\right]^{-2}\right\}, \quad (1)$$

which depends on the shock speed in downstream flow frame, u_2, particle speed, v, and the inverse wave-amplitude parameter, ϵ. Here $\tilde{v} = \epsilon\ v/u_2$ is the normalized particle velocity. The only free parameter of this model is rather well constrained, since $0.3 \lesssim \epsilon \lesssim 0.4$ for strong shocks (Malkov and Völk, 1998). Due to the exponential cut off in a thermal velocity distribution, however, the injection rate depends rather sensitively on the value of ϵ. We refer to particles populating the velocity range where $\partial\tau_{\rm esc}/\partial p \neq 0$ as an "injection pool". A proportion of the particles in the injection pool just above the Maxwellian tail can leak upstream and participate in Fermi acceleration.

Thus, in the new CR/AMR code the diffusive flux of suprathermal particles across the shock to the upstream region is filtered by the transparency function so that the probability for leakage is zero below the injection pool, then increases to unity above the injection pool. The rate of particles injected into the Fermi process is then proportional to the convolution of $\partial\tau_{\rm esc}/\partial p$ with $f(p)$ of Maxwellian tail.

4 Results

Following Gieseler et al. (2000), we adopt the following definitions for the injection and acceleration efficiencies. The fraction of particles that has been swept through the shock after the time t, and then injected into the CR distribution is given by

$$\xi(t) = \frac{\int \mathrm{d}x \int f_{\rm cr}(p,x,t)\mathrm{d}^3\mathrm{p}}{n_1 u_1\, t} \tag{2}$$

where $f_{\rm cr}$ is the CR distribution function and $n_1 u_1$ is the particle number flux far upstream. The fraction of initial total energy flux through the shock that is transferred to CRs is given by

$$\eta(t) = \frac{\frac{\gamma_c(t)}{\gamma_c(t)-1} u_{\rm d}(t) P_{\rm c}(t)}{\frac{1}{2}\rho_{\rm d} u_{\rm d}^3 + \frac{\gamma_g}{\gamma_g - 1} u_{\rm d} P_{\rm g,d}}\,, \tag{3}$$

where $u_{\rm d}$ is the initial downstream plasma velocity in the upstream rest frame.

The dynamics of the CR modified shock depends on four parameters: the gas adiabatic index, $\gamma_{\rm g} = 5/3$, gas Mach number of the shock, $M = V_s/c_s$, $\beta = u_o/c$, and the diffusion coefficient, κ. Here u_o is the velocity normalization constant corresponding the upstream flow velocity. For all simulations we present here u_o =5000 kms^{-1}. We assume a Bohm type diffusion coefficient, $\kappa_{\rm B} = \kappa_o p^2/(p^2+1)^{1/2}$, where p is expressed in units of $m_{\rm p}c$. The length and the time variables scale with κ_o through the diffusion length and time defined as $r_o = \kappa_o/u_o$ and $t_o = \kappa_o/u_o^2$. Thus we do not need to choose a specific value for κ_o, as long as we adopt r_o and t_o as normalization constants. We considered five values for Mach number, $M = 3$, 5, 10, 20, and 30 for the initial shock jump by adjusting the preshock gas pressure. The initial jump conditions in the rest frame of the shock for all test problems are: $\rho_1 = 1$, $u_1 = -1$, $P_{g,1} = 7.5 \times 10^{-1}/(1.25M^2 - 0.25)$ in the upstream region and $\rho_2 = r$, $u_2 = -1/r$, $P_{g,2} = 7.5 \times 10^{-1}$ in downstream region, where the compression ratio is $r = 4M^2/(M^2+3)$. The simulations were carried out on a base grid with $\Delta x_0 = 3.2 \times 10^{-3}$ using $l_{\rm max} = 5$ additional grid levels, so $\Delta x_5 = 10^{-4}$ on the finest grid. The number of refined cells around the shock is $N_{rf} = 200$ on the base grid and so there are $2N_{rf} = 400$ cells on each refined level.

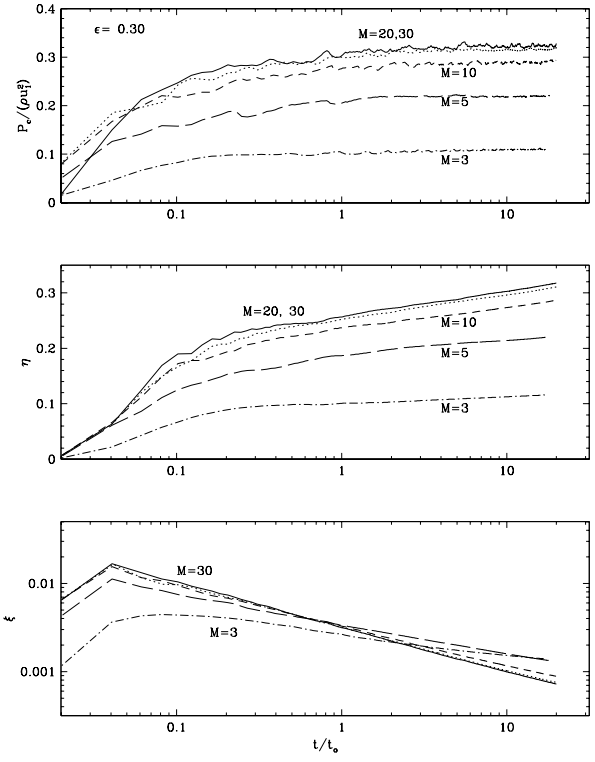

Fig. 3. Top: Postshock CR pressure in units of ram pressure, Middle: Acceleration efficiency $\eta(t)$, Bottom: Injection efficiency $\xi(t)$ for $M = 3$, 5, 10, 20 and 30 shocks for the inverse wave-amplitude parameter, $\epsilon = 0.3$.

Fig. 1 shows time evolution of the CR modified shock structure for a $M = 30$ shock with $\epsilon = 0.3$. This shows how the precursor grows and the flow structure is modified as CRs are accelerated. Evolution of the CR distribution function, at the shock, represented as $g = p^4 f(p)$ is given for the same shock in Fig. 2. The transparency function at $t/t_o = 0$ and 20 is also plotted for reference. For $p/m_{\rm p}c >> 1$ the quantity g is proportional to the partial pressure per unit of log momentum. Just above the injection pool, the distribution function changes smoothly from a Maxwell distribution to an approximate power–law whose index is close to the test–particle slope. As the postshock temperature decreases due to energy transfer to CRs, the Maxwell distribution shifts to lower momenta, but the transparency function shifts only slightly to lower momenta. The shift in the transparency

function, $\tau_{\rm esc}(v, u_2)$, is tied to the decrease of the shock velocity u_2; i.e., to increased compression, as the precursor grows more significantly in time. As a result, the injection rate decreases over time following an initial "start-up" increase when the postshock temperature is high. We note that the particle distribution does not evolve as a simple power-law or concave curve, but, instead, it depends on the injection history.

Fig. 3 shows how the CR pressure at the shock, and the acceleration/injection efficiencies, η and ξ, evolve for shocks with different Mach numbers when the inverse wave-amplitude paramter $\epsilon = 0.3$ is adopted. The average value of η in the postshock region within a distance $(u_2 t)/2$ of the shock is plotted. While a fraction of particles injected earlier continue to be accelerated to higher momenta and to add to P_c, the injection rate for new particles decreases as the postshock gas cools, resulting in steady values of the postshock P_c. For all Mach numbers the postshock P_c increases until $p_{\rm max}/m_{\rm p}c \sim 1$, and then stays at a steady value afterwards. So the ratio of the postshock CR pressure to the ram pressure evolves in these shocks to the range roughly from 0.1 to 0.3. This ratio becomes 0.32 for strong shocks with $M \gtrsim 20$, independent of Mach number. Although P_c stays almost steady for $\tilde{t} = t/t_o > 1$, the acceleration efficiency η slowly increases because of decrease of γ_c due to increasing dominance of relativistic particles. After the initial adjustment period of $\tilde{t} < 0.05$, the injection rate can be fitted as a power-law form for the shock models considered here, $\xi \sim 0.01(\tilde{t}/0.1)^{-\alpha}$ for $\tilde{t} < 20$, where $0.2 \lesssim \alpha \lesssim 0.5$ with larger values for higher M. Injection is slower initially for lower Mach number shocks, and so the postshock temperature and injection rate decrease more slowly. According to a much longer simulations to $\tilde{t} \sim 1000$ but with a lower spatial resolution, the power-law decrease of ξ flattens out later. General trends shown in Fig. 3, that is, steady values of P_c, increase of η, decrease of ξ in time, seem valid in the longer simulation.

We have also consider the models with $\epsilon = 0.35$. The main results are similar to the models with $\epsilon = 0.3$, but the injection rate is slightly higher and so values of postshock P_c are higher by about 18%.

5 Discussion

We have shown through self-consistent numerical simulations that the "thermal leakage" injection process at quasi-parallel CR shocks is regulated by the convolution of the population in the high energy tail of the Maxwell velocity distribution and the function $\tau_{\rm esc}(p, u_2)$, so it depends strongly on the physical properties of the postshock gas, that is, the postshock flow speed and the gas temperature. Initially the injection rate increases to $\xi \sim 0.01$ until $t \sim t_{\rm acc}(p_{\rm inj})$, the acceleration time scale of the injection momenta. Afterwards it decreases as the postshock gas cools and the Maxwell distribution shifts to lower momenta due to significant initial energy transfer to CRs. For stronger shocks the initial injection rate is higher, so the postshock temperature decreases faster, resulting in a lower injection rate in later evolution compared to weaker shocks. The injection rate, defined as the fraction of the particles passed through the shock that are accelerated to form the CR population, can be fitted as a power-law form, $\xi \sim 0.01(\tilde{t}/0.1)^{-0.5}$ up to $\tilde{t} \sim 20$ for strong shocks of $M \gtrsim 20$ and the inverse wave-amplitude parameter $\epsilon = 0.3$.

Although our CR/AMR code is much more efficient that conventional codes, we have so-far integrated our models only until the maximum momentum reaches about $\sim 10 m_{\rm p}c$, since computational requirements of using a Bohm type diffusion model are still substantial. However, we expect the following features to remain valid beyond our simulation time:

1. In the strong shock limit of $M \gtrsim 20$, significant physical processes such as the injection and acceleration seem independent of the shock Mach number, while they are sensitively dependent on M for $M \lesssim 10$.

2. Although some particles injected early in the shock evolution continue to be accelerated to higher energies, the postshock CR pressure reaches a steady value, because the injection rate for new particles decreases. For the $M \gtrsim 20$ shock model, this converges to a maximum conversion factor of $P_c \sim 0.32 \rho_1 u_1^2$ for $\epsilon = 0.3$, where $\rho_1 u_1^2$ is the ram pressure of far upstream flow.

3. In the strong shock limit the shock is significantly modified, yet not CR dominated, because of the previous point.

These findings are different from previous perspectives in which strong shocks can be CR dominated and CRs can absorb almost all of the ram pressure of shocks under the assumption of constant injection rate. In future studies we will extend our simulations to much longer times to confirm our tentative conclusions presented in this work.

Acknowledgements. HK was supported by Korea Research Foundation Grant (KRF-2000-015-DP0448). TWJ is supported by the University of Minnesota Supercomputing Institute, by NSF grant AST-9619438 and by NASA grant NAG5-5055. The numerical calculations were performed on an GS320 system of the KISTI Supercomputing center.

References

Bell A.R., MNRAS 182, 147, 1978
Berger, J. S., and LeVeque, R. J. SIAM J. Numer. Anal., 35, 2298, 1998
Drury, L. O'C., Rept. Prog. Phys., 46, 973, 1983
Gieseler U.D.J., Jones T.W., and Kang H., A&Ap, 364, 911, 2000
Kang, H., Jones, T. W., LeVeque, R. J., and Shyue, K. M, ApJ, 550, 737, 2001.
LeVeque, R. J., and Shyue, K. M., SIAM J. Scien. Comput. 16, 348, 1995
Malkov M.A. Phys. Rev. E, 58, 4911, 1998
Malkov M.A., and Völk H.J., 1998, Adv. Space Res. 21, 551
Quest K.B., J. Geophys. Res. 93, 9649, 1998
Skilling, J., MNRAS, 172, 557, 1975